

Development of a Renewable Energy Forecasting Strategy Based on Numerical Weather Prediction for the Cold Ironing System at the Port of Ancona, Italy



Daniele Colarossi*, Valerio D'Alessandro, Luca Giammichele, Matteo Falone, Renato Ricci

Department of Industrial Engineering and Mathematical Sciences, Università Politecnica delle Marche, Ancona 60131, Italy

Corresponding Author Email: d.colarossi@univpm.it

Copyright: ©2024 The authors. This article is published by IIETA and is licensed under the CC BY 4.0 license (<http://creativecommons.org/licenses/by/4.0/>).

<https://doi.org/10.18280/ijepm.090401>

Received: 15 October 2024

Revised: 14 November 2024

Accepted: 30 November 2024

Available online: 31 December 2024

Keywords:

cold ironing, WRF, energy forecasting, solar energy, wind energy

ABSTRACT

Since renewable energy sources have an intermittent nature, forecasting strategies are increasingly important. In parallel, ports are characterized by large energy demands, especially from berthed ships. Cold ironing systems have already been proven to reduce their environmental impact by connecting ships to the electricity grid and allowing them to switch off their auxiliary engines in port. In this work, a local energy production, consisting of photovoltaic, wind turbines, and an energy storage system, is proposed to cover the energy demand of ships. In addition, an energy forecasting strategy is presented, where the solar and wind energy potential is provided by the Weather and Research Forecasting (WRF) mesoscale model. By forecasting the energy production for the following day, the storage system can be charged from the grid at night, namely in off-peak periods, reducing the pressure on the grid in on-peak periods. The methodology is tested on the port of Ancona (Italy). Results show that energy production can directly cover 54% of energy demand, and up to 70% by adding the storage system. The forecasting strategy reduces the energy withdrawn during the daytime by 24.9% and increases that during the nighttime by 18.9%, proving the effectiveness of the proposed strategy.

1. INTRODUCTION

In the global pursuit of sustainable energy solutions, the imperative for accurate forecasting methodologies of renewable energy production has become increasingly important [1]. As the world grapples with the challenges of climate change, it is imperative to acknowledge the significant contributions to global pollution, including emissions from maritime activities in ports [2]. Recent data suggests that maritime transport alone accounts for approximately 2-3% of global greenhouse gas emissions, with port operations playing a notable role in this contribution [3]. The operations in ports contribute to local air pollution, adding to the broader environmental concerns posed by greenhouse gas emissions [4]. This underscores the urgent need for sustainable alternatives to mitigate the environmental impact of maritime transportation. It is worth mentioning that the more the port is close to urban areas, the more the environmental impact and the pollution in the area will be [5].

The adoption of renewable energy sources such as wind, solar, and hydroelectric power offers a promising solution to face climate change and reduce pollution from port activities [6]. Additionally, implementing cold ironing systems in ports, also known as shore power or Alternative Maritime Power (AMP) [7], can significantly reduce emissions by providing electrical power to ships while they are berthed, thereby eliminating the need for diesel engines, usually used on traditional ships [8]. Cold ironing effectively allows to shut

down of auxiliary engines on ships, which are typically used to power various onboard activities such as lighting, ventilation, and refrigeration. By connecting ships to onshore electrical grids, cold ironing enables vessels to rely on cleaner energy sources while in port, thereby reducing air pollution and greenhouse gas emissions [9]. In addition, the environmental performance of a cold ironing system depends on the electrical mix from which the energy is withdrawn. If a low-quality energy mix is used, the environmental benefit will not be ensured. Accordingly, the performance can be maximized when the cold ironing is powered by renewable energy sources [10].

It is well known that renewable energy sources, such as solar and wind energy, have an inherently intermittent nature. Accordingly, accurate short-term weather forecasting plays a pivotal role in the efficient management of renewable energy production [11]. This way, especially when the energy demand is strongly intermittent, the advanced knowledge of the energy demand and production can be utilized to increase the management efficiency of microgrids, better exploiting the energy storage systems, with strategies such as peak shaving and energy arbitrage [12]. Among the methodologies for energy production forecasts, the Weather Research and Forecasting (WRF) model [13] stands out as a powerful tool for predicting meteorological conditions with high spatial and temporal resolution [14]. Developed by the National Center for Atmospheric Research (NCAR), the WRF model is widely used in both research and operational forecasting due to its

ability to simulate atmospheric processes across various spatial and temporal scales [15]. Unlike traditional weather models, WRF employs three-dimensional domains, allowing for a more comprehensive representation of atmospheric dynamics and interactions. By incorporating advanced numerical techniques, parameterizations, and observational data assimilation, WRF enables stakeholders to anticipate energy demand and production patterns with enhanced precision. A WRF model can be used to both wind [16] and solar energy predictions [17], and this would allow to forecast the energy production from renewable sources. This could be implemented to support a cold ironing system [18].

In this context, this paper presents a predictive model based on the WRF mesoscale model [19], to estimate the energy production from renewable sources and to increase the management efficiency of a cold ironing system. Power plants consist of both wind turbines and photovoltaic panels and are flanked by an energy storage system to eventually store a surplus of energy production. The latter is used to meet the energy demand of ferry ships docked at the port of Ancona, used as a case study [20]. The aim is to replace the onboard diesel generators of ships with an onshore power supply, as expected by the cold ironing systems. The ferry traffic at the port was analyzed on an hourly basis.

The paper is organized as follows: in Section 2 the proposed system and forecasting methodology are widely described, in Section 3 results are shown and discussed and in Section 4 conclusion and main findings are listed.

2. MATERIAL AND METHODS

The methodology proposed consists of different steps:

- (1) Evaluation of the energy demand by berthed ships.
- (2) Evaluation of the energy production by renewable energy plants.
- (3) Implementation of the control loop to compare energy production and demand on an hourly basis.
- (4) Implementation of the energy forecasting strategy.

The ferry traffic of the port of Ancona (Italy) was taken as a case study, with methodology applicable to all ship types and locations.

2.1 Energy demand

Ferries are chosen due to their regular port calls and moderate energy demand compared to cruise ships, which have a higher energy demand (generally up to 10 MW), and container ships, which have a lower energy demand (up to 1 MW).

The hourly energy demand was calculated for each ship, based on a typical weekly pattern. From these, the monthly profile is reconstructed as a sequence of typical weeks. This is acceptable since ferries show a regular schedule of arrivals and departures in port.

The overall energy demand profile, for all ships, is calculated considering the contemporaneity of ships in port. The overall power required at a certain time is the sum of the energy demand of the number of ships present in port at that time. The period analyzed in this work is February 2024. Table 1 reports the list of ships analyzed, and for each of them, the power required at berth and the total time spent in port are listed.

It is worth noting that not all the ferries stayed at the port during February. Figure 1 shows the reconstruction of the hourly energy demand of the contemporaneity of ships, during February 2024.

Table 1. Ferry ships considered at the port of Ancona

	Average Power (kW)	Total Time (h)	Nº Calls
Ship 1	1600	80	4
Ship 2	1000	136.3	12
Ship 3	1000	76.6	4
Ship 4	2200	50.6	16
Ship 5	2200	46.3	16
Ship 6	1200	0	0
Ship 7	800	158.7	8
Ship 8	350	24.3	4
Ship 9	600	0	0
Ship 10	800	0	0

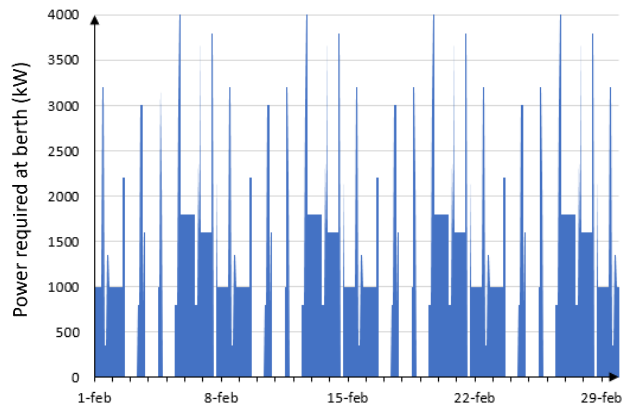


Figure 1. Temporal evolution of the energy demand (February 2024)

2.2 Energy production

The proposed energy production strategy integrates both photovoltaic (PV) and wind turbine systems to meet the electricity demand of berthed ships. The renewable energy resources, both solar radiation and wind speed, are determined by WRF simulations. Then the obtained results were used to calculate the energy produced by the power plants.

WRF produces mesoscale forecasts by integrating fluid flow equations and parameterizing unresolved processes. These include microphysics, radiation (longwave and shortwave), planetary boundary layer, land surface, and convection (for grid spacing above 4 km).

The modeling domains are centered on the city of Ancona (Italy) and consist of five nested domains, with a grid spacing of 24300 m, 8100 m, 2700 m, 900 m, and 300 m. All domains have 31×31 points on the horizontal spatial domain, and 27 levels in the vertical direction. The time step for all simulations was set to 80 seconds and the output was visualized each 4 minutes. Data for the boundary and initial conditions for all downscaling were taken from the Global Forecasting System (GFS) database. The latter is a database of meteorological data obtained through a reanalysis process, performed with a large resolution worldwide or over wide regions. Then the WRF model allows us to solve the equations on the domain set. Each simulation was initialized at 00:00 of each day over the period considered and covered the following 48 hours. Figure 2 shows the WRF domains.

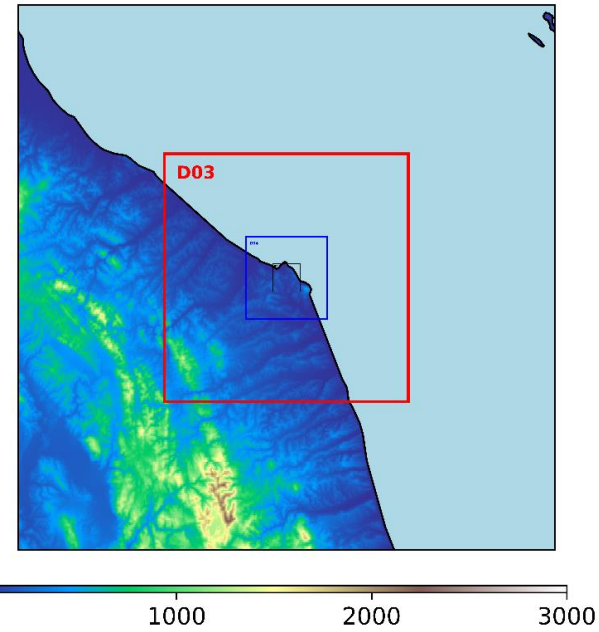


Figure 2. Domains for the simulation on Ancona (Italy) with altitude color map (meters) latitude=43.586505; longitude=13.515598

Once the renewable energy resources are estimated, the output power for both photovoltaic plants and wind turbines can be calculated. Regarding the photovoltaic system, the required parameters are the solar irradiance and the ambient temperature. The output power of the PV system (P_{PV}) is determined by Eq. (1):

$$P_{PV} = P_r \cdot f_{PV} \cdot \left(\frac{G_t}{G_{T, STC}} \right) \cdot \left[1 + \alpha_p \cdot (T_c - T_{c, STC}) \right] \quad (1)$$

where, P_r represents the rated capacity of the PV plant, f_{PV} denotes the PV derating factor, G_t stands for the solar radiation incident on the PV array in the current time step, $G_{T, STC}$ is the incident radiation at standard test conditions, α_p represents the temperature coefficient of power, T_c indicates the PV cell temperature in the current time step, and $T_{c, STC}$ denotes the PV cell temperature under standard test conditions. It is worth remembering that the Standard Test Conditions (STC) correspond to a solar radiation of 1000 W/m², an ambient temperature of 25°C and an air mass of 1.5. The PV cell temperature (T_c) is expressed as a function of ambient temperature (T_a), incident solar radiation (G_t), and the panel's operative temperature ($NOCT$), as Eq. (2):

$$T_c = T_a + \frac{(NOCT - 20)}{800} \cdot G_t \quad (2)$$

In this work, a temperature coefficient of power α_p equal to -0.005 and a NOCT equal to 45°C were used, as typical values of monocrystalline silicon panels.

For the wind turbine system, the output power (P_w) is calculated using the relevant equations incorporating factors such as rated capacity, wind speed, and turbine characteristics. While the specific formula may vary depending on turbine models and attributes, it typically involves parameters like air density, rotor diameter, and wind speed cubed, denoted by Eq. (3):

$$P_w = \frac{1}{2} \cdot \rho \cdot C_p \cdot A \cdot w_s^3 \quad (3)$$

where, P_w is the power produced by the wind turbine, ρ is the air density, A represents the rotor swept area, C_p denotes the power coefficient, and w_s indicates the wind speed. Figure 3 shows the power curve of the wind turbine considered in this work. It is a wind turbine with a rated power of 2050 kW and a rated wind speed of 12 m/s.

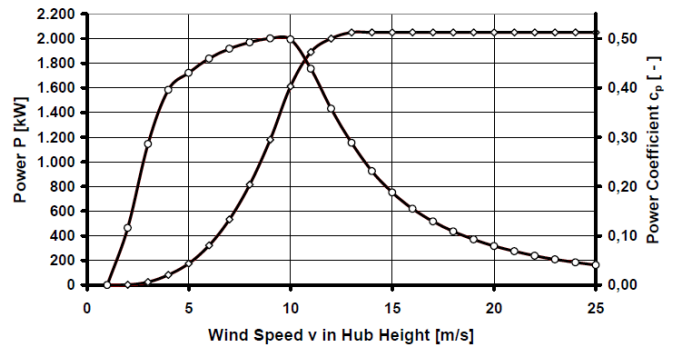


Figure 3. The overall layout of the proposed system

The performance of the wind turbine is influenced by wind speed fluctuations and meteorological conditions, necessitating the employment of mathematical models to forecast output under various wind scenarios.

2.3 Control loop

A control loop was developed and implemented in MATLAB, to determine the energy flows among the different components of the proposed system. In particular, the latter consists of photovoltaic plants and wind turbines as energy sources, an energy storage system, and berthed ships as energy load. Figure 4 shows the overall layout. Both photovoltaic and wind energy can be used to cover the energy demand of ships, to charge the energy storage system, or to deliver energy to the electrical grid, in case of energy surplus or when the energy storage is fully charged. Alternatively, in the absence of energy production from power plants, the energy demand can be satisfied with the energy stored, if present, or directly from the electrical grid.

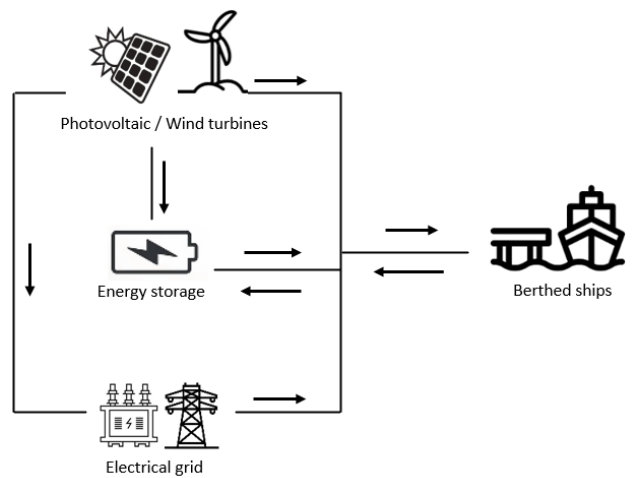


Figure 4. Overall layout of the proposed system

The control loop allows to evaluate how the energy demand is covered. The model aims to allocate the share of energy demand to the PV/wind turbines, to the storage system or to the grid, depending on the energy availability at that certain time. The working mechanism is the following. At each time step, the model requires as input the environmental parameters, such as the solar irradiance (G_T), the ambient temperature (T_a) and the wind speed (W_s), and the power consumption of ships (P_i).

Then, the model operates by comparing the energy demand and production on an hourly basis. It calculates the PV output using Eqs. (1) and (2), and wind turbines output using Eq. (3). When the energy production is lower than the energy demand, the model calculates the energy deficit, while on the contrary, namely when the energy production is higher than the energy demand, the energy surplus is calculated.

In the first case, the model checks the State of Charge (SoC) of the storage system to verify whether it can cover the energy deficit. If the energy deficit is higher than the SoC, the further deficit is withdrawn from the electrical grid.

In the second case, in presence of an energy surplus, the model checks whether it can be stored or, when the energy storage system is fully charged, the surplus is supplied to the electrical grid.

The diagram flow in Figure 5 shows the logic of the proposed loop, which is repeated on an hourly basis over the considered period.

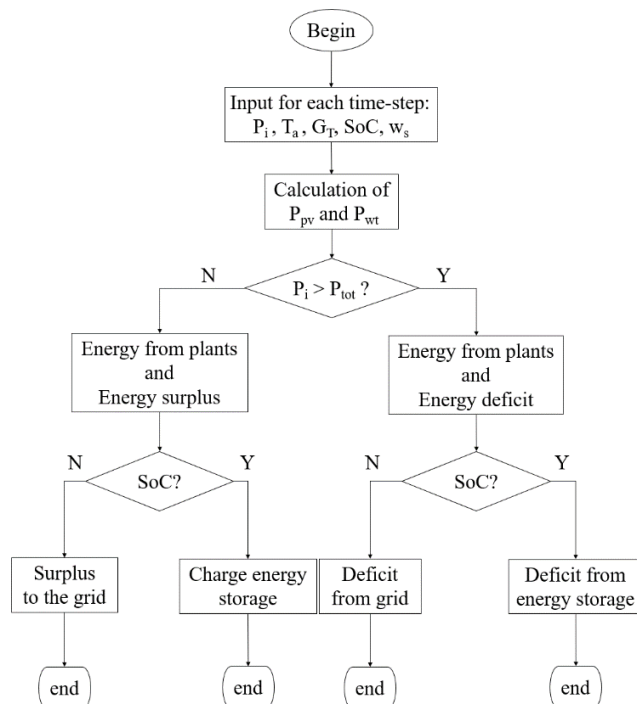


Figure 5. Diagram flow of the proposed system

2.4 Energy forecasting strategy

The proposed strategy aims to return a more self-sufficient cold ironing system, in terms of energy exchanges with the electricity grid. The use of renewable energy sources is unprogrammable and unstable, and accordingly, it can be used only when produced.

The proposed strategy for energy management involves a strategic assessment of renewable energy production and anticipated demand. The workflow is the following:

- (1) WRF simulations.
- (2) Solar and wind data extraction.
- (3) Control loop and forecasting strategy.

WRF simulations run every day to predict the following 48-hour weather conditions. The procedure automatically starts at 5 AM each day. This is because it generally takes 4 hours for the NCAR to release GFS weather data, which contains the initial and boundary conditions for the WRF simulations. Once the data are downloaded, the simulation begins and lasts around 3 hours.

At 10 AM the outputs of the simulation are taken as input for the post processing. This is performed through the NCL scripting language, developed by the Computational and Information Systems Lab at the NCAR. The aim is to extract the weather conditions at any point of the domain, namely the wind data at the desired height and solar data at the ground surface.

Each evening at 8 PM, the forecasting strategy is implemented by analyzing the projected output from renewable sources, both solar and wind, as well as the energy demand of ships docked at the port for the following day. This step is necessary to determine whether the next day there will be an energy surplus of production compared to the energy demand or an energy deficit. The model focuses only on the latter case, which means that the energy demand of the following day is higher than the energy production. In this scenario, the model calculates the evolution of the state of charge of the storage system, to verify the possibility to charge the storage during the night-time. This allows the storage system to be charged with energy taken from the grid at a lower price. The new overall layout of the proposed system appears as in Figure 6.

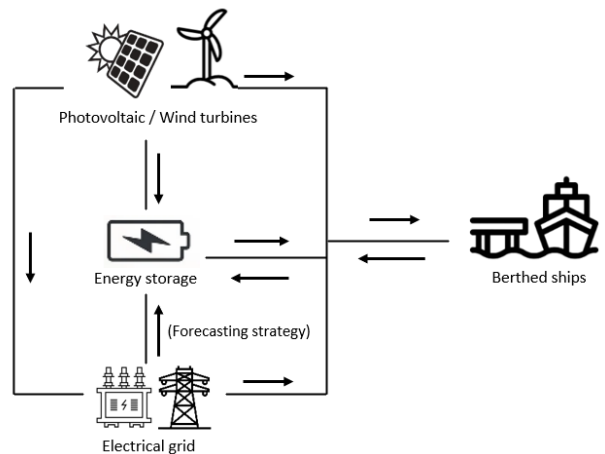


Figure 6. Revised layout with energy forecasting strategy

3. RESULTS AND DISCUSSION

3.1 Validation of the WRF simulations

Before implementing the energy forecasting strategy to the cold ironing system, results obtained from solar and wind energy estimations, through WRF simulations, need to be validated. In the absence of experimental data over the simulated period, February 2024, in this work the validation process will consist of two phases:

- (1) Validation of a hindcasting model with experimental data. The latter are available over one year, 2010, in

Lesina (Italy).

- (2) Once the hindcasting model is validated, the same configuration will be used to simulate the period of interest, February 2024, and compared with the data obtained by the forecasting simulations.

A hindcasting simulation involves using the WRF model to simulate past weather conditions. Instead of forecasting future weather, the model is "hindcasted" or runs backward in time to recreate past weather events. A comparative analysis between numerical results and experimental data was performed. The experimental data were collected from an anemometric tower installed in Lesina (Italy), in 2010. The tower was equipped with the instrumentation for wind energy assessment at different levels, namely 40 m, 60 m, 80 m, and 100 m.

Figure 7 shows the wind roses of experimental (a) and numerical (b), at a height of 60m from the terrain level. A wind rose is a graphical tool used to measure wind direction and speed from an anemometric tower or a wind dataset. It represents the frequency and intensity of wind blowing from different directions over a specific period. As seen from the figure, the two wind roses are similar, and the predominant wind direction is south for the numerical scenario, while slightly southeast with the experimental data. Regarding the wind speed, the different colors highlight the ranges of wind speed. It can be concluded that the wind speeds are similar, with the numerical scenario that shows lower average wind speeds over the year. Table 2 summarizes the average wind speed at the different levels.

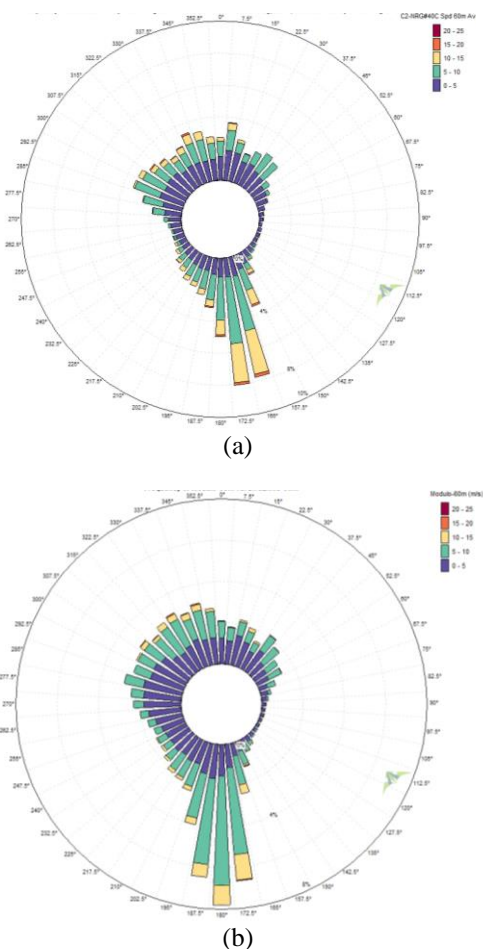


Figure 7. (a) Wind roses of experimental, (b) Wind roses of numerical

Table 2. Average wind speed at the different levels (Lesina, 2010)

Level	Hindcasting	Anemometric Tower
40 m	4.98 m/s	5.55 m/s
60 m	5.49 m/s	5.94 m/s
80 m	5.83 m/s	6.27 m/s
100 m	6.05 m/s	6.4 m/s

The comparison between forecasting and hindcasting simulations can be considered as the latter was validated many times in literature. In this work, the period analyzed is February 2024. The hindcasting simulations were performed under the same conditions as the forecasting ones, namely the grid sizes and resolutions, the time step, and the vertical levels. The comparison was made in terms of average wind speed over the entire period and the standard deviation. As shown in Table 3, the forecasting simulations can be considered validated.

Table 3. Hindcasting and forecasting comparison (February 2024)

	Average Speed (m/s)	Standard Deviation (m/s)
Hindcasting	4.819	2.245
Forecasting	4.835	2.289

3.2 Comparison of the different scenarios

Different scenarios were simulated to investigate and prove the effectiveness of the proposed forecasting strategy.

Cases:

- (1) Simple cold ironing system. The energy demand is always covered by the electricity grid.
- (2) Cold ironing with local energy production. The energy demand can be covered whether by local energy production or by the electricity grid.
- (3) Cold ironing with local energy production and energy storage system. In addition to the previous case, the energy storage system can cover the energy demand in the absence of renewable energy production.
- (4) Cold ironing with local energy production, energy storage system, and energy forecasting strategy. The latter allows us to predict the energy and production and withdraw in advance during the off-peak period.

Table 4 shows the sizes of the power plants and the energy storage used for the simulations. It is worth citing that the 6150 kW of wind turbines corresponds to three turbines hypothesized, 2050 kW each.

Table 4. Power plants and storage systems simulated

	Rated Power (kW)	Capacity (kWh)
Photovoltaic plant	4500	-
Wind turbines	6150	-
Energy storage system	-	6000

Results are analyzed in terms of percentage coverage of the energy demand. Figure 8 shows how the energy demand is covered by the different components of the proposed scenarios. In the first one, Figure 8 (a), there is no local energy production, and the energy production is fully satisfied by the electricity grid. In the second scenario Figure 8 (b), namely with the

addition of the local energy production, the energy demand can be directly met by the energy produced, and this share turns out to be 54%, while the remaining share (46%) is covered by the electricity grid. By adding the energy storage system Figure 8 (c), the third scenario, the energy surplus can be stored and then used in case of an energy production deficit. The share from renewable energy remains the same (54%), while the share of energy from the grid decreases by 16% (from 46% to 30%), which corresponds to the share provided by the energy storage system.

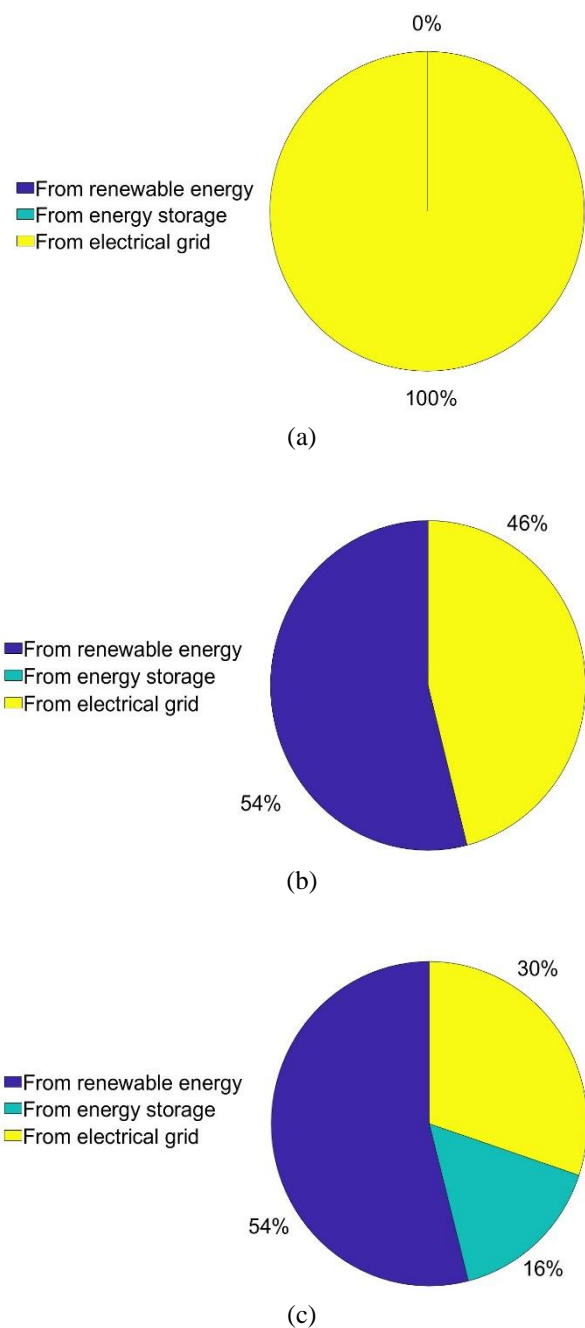


Figure 8. Energy demand coverage for the different scenarios

3.3 Energy forecasting strategy

The energy forecasting strategy aims to reduce the energy taken from the grid during the on-peak period. In fact, during the daytime, there is usually a peak of energy production from

renewable sources, mainly due to the daily profile of solar radiation. The proposed strategy aims to shift the share of energy withdrawn from the daytime to the night-time.

Figure 9 shows, for each scenario, how the energy taken from the grid is allocated during the day. More in detail, the day-time period corresponds to the 8:00/20:00 time range, while the night-time period corresponds to the 20:00/8:00 time range.

As expected, results show that, by adding the local energy production (scenario 2) and the energy storage system (scenario 3), the overall share of the energy taken from the grid decreases both during the daytime and night-time. The proportions of the decrease are a consequence of the availability of renewable resources, both solar radiation and wind speed and of the daily distribution of the energy demand of ships.

The fourth scenario, the one implementing the forecasting strategy, shows a reduction in the energy withdrawn during the daytime (24.9%) and an increase in the energy withdrawn during the night-time (18.9%). This proves that the proposed forecasting strategy turns out to be valid to reduce the pressure on the grid during the on-peak period. In addition, this could lead to a reduction in operational costs, due to the lower cost of energy in the night-time than in the daytime.

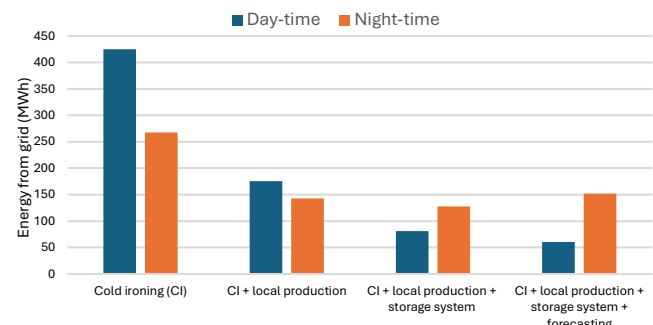
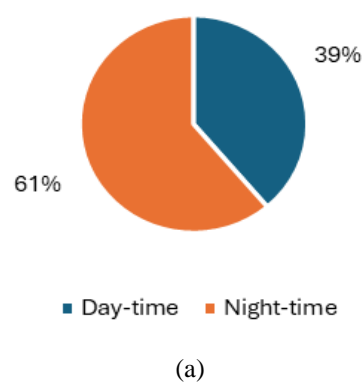


Figure 9. Energy withdrawal distribution for the different scenarios

To better investigate the effectiveness of the proposed focusing strategy, Figure 10 highlights the third and fourth scenarios, namely without and with forecasting strategy. It can be seen that by adding the strategy the day-time energy withdrawn from the electricity grid is reduced from 39% to 29%. Accordingly, the share during the night-time is increased from 61% to 71%. This proves the effectiveness of the proposed strategy, reducing the pressure on the grid during the on-peak period and the cost of energy withdrawn.



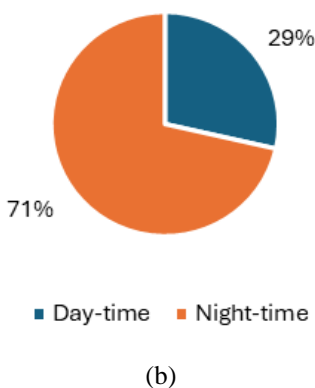


Figure 10. (a) Energy withdrawn allocation without forecasting strategy, (b) Energy withdrawn allocation with forecasting strategy

4. CONCLUSIONS

This paper presents an energy forecasting strategy based on the WRF mesoscale model. The latter is used to predict, through a series of 48-hour weather forecasts, the energy potential of both solar and wind power plants. The energy production aims to cover the energy demand of berthed ships at the port of Ancona (Italy), used as a case study, with an onshore power supply, as expected from the cold ironing systems. The energy demand is analyzed on an hourly basis.

The forecasting strategy consists of determining each evening the energy production for the following day. In case of a deficit, the storage system is charged at night with energy taken from the grid at a lower price.

The main findings of this work can be summarized as follows:

(1) A local energy production from 4500 kW of photovoltaic and 6150 kW of wind turbines can directly cover 54% of the energy demand of ships, which is strongly intermittent.

(2) By adding an energy storage system with a capacity of 6000 kWh, the self-sufficiency of the overall system increases up to 70%.

(3) The proposed forecasting strategy can help to reduce the pressure on the electrical grid during the on-peak period. The energy withdrawn during the daytime is reduced by 24.9%, and that during the night-time is increased by 18.9%.

Future research will be developed, for instance, the validation of the forecasting output with experimental data, such as with an anemometric tower. In addition, the optimal sizing of the system's components could be investigated, or the influence of the uncertainties in both energy potential assessment and energy demand of ships.

REFERENCES

- [1] Khaleel, M., Yusupov, Z., Alderoubi, N., Abdul_jabbar, R.L., Elmnifi, M., Nassar, Y., Majdi, H.S., Habeeb, L.J., Abulifa, S. (2024). Evolution of emissions: The role of clean energy in sustainable development. *Challenges in Sustainability*, 12(2): 122-135. <https://doi.org/10.56578/cis120203>
- [2] Apriantoro, M.S., Dartim, Andriyani, N. (2024). Bibliometric analysis of carbon capture and storage (CCS) research: Evolution, impact, and future directions. *Challenges in Sustainability*, 12(2): 152-162. <https://doi.org/10.56578/cis120205>
- [3] International Maritime Organization. Highlights and Executive Summary of the Fourth IMO GHG Study 2020 HIGH. <https://www.imo.org/en/ourwork/Environment/Pages/Fourth-IMO-Greenhouse-Gas-Study-2020.aspx>, accessed on Jan. 17, 2024.
- [4] Bakar, N.N.A., Bazmohammadi, N., Vasquez, J.C., Guerrero, J.M. (2023). Electrification of onshore power systems in maritime transportation towards decarbonization of ports: A review of the cold ironing technology. *Renewable and Sustainable Energy Reviews*, 178: 113243. <https://doi.org/10.1016/j.rser.2023.113243>
- [5] Dragović, B., Tzannatos, E., Tselenitis, V., Meštrović, R., Škurić, M. (2018). Ship emissions and their externalities in cruise ports. *Transportation Research Part D: Transport and Environment*, 61: 289-300. <https://doi.org/10.1016/j.trd.2015.11.007>
- [6] Rolán, A., Manteca, P., Oktar, R., Siano, P. (2019). Integration of cold ironing and renewable sources in the barcelona smart port. *IEEE Transactions on Industry Applications*, 55(6): 7198-7206. <https://doi.org/10.1109/TIA.2019.2910781>
- [7] Sciberras, E.A., Zahawi, B., Atkinson, D.J. (2015). Electrical characteristics of cold ironing energy supply for berthed ships. *Transportation Research Part D: Transport and Environment*, 39: 31-43. <https://doi.org/10.1016/j.trd.2015.05.007>
- [8] Lou, H., Hao, Y., Zhang, W., Su, P., Zhang, F., Chen, Y., Li, Y. (2019). Emission of intermediate volatility organic compounds from a ship main engine burning heavy fuel oil. *Journal of Environmental Sciences*, 84: 197-204. <https://doi.org/10.1016/j.jes.2019.04.029>
- [9] Spengler, T., Tovar, B. (2021). Potential of cold-ironing for the reduction of externalities from in-port shipping emissions: The state-owned Spanish port system case. *Journal of Environmental Management*, 279: 111807. <https://doi.org/10.1016/j.jenvman.2020.111807>
- [10] Colarossi, D., Lelow, G., Principi, P. (2022). Local energy production scenarios for emissions reduction of pollutants in small-medium ports. *Transportation Research Interdisciplinary Perspectives*, 13: 100554. <https://doi.org/10.1016/j.trip.2022.100554>
- [11] Ma, J., Ma, X. (2018). A review of forecasting algorithms and energy management strategies for microgrids. *Systems Science & Control Engineering*, 6(1): 237-248. <https://doi.org/10.1080/21642583.2018.1480979>
- [12] Aslam, S., Khalid, A., Javaid, N. (2020). Towards efficient energy management in smart grids considering microgrids with day-ahead energy forecasting. *Electric Power Systems Research*, 182: 106232. <https://doi.org/10.1016/j.epsr.2020.106232>
- [13] Zhao, J., Guo, Y., Xiao, X., Wang, J., Chi, D., Guo, Z. (2017). Multi-step wind speed and power forecasts based on a WRF simulation and an optimized association method. *Applied Energy*, 197: 183-202.
- [14] Jacondino, W.D., da Silva Nascimento, A.L., Calvetti, L., Fisch, G., Beneti, C.A.A., da Paz, S.R. (2021). Hourly day-ahead wind power forecasting at two wind farms in northeast Brazil using WRF model. *Energy*, 230: 120841.

<https://doi.org/10.1016/j.energy.2021.120841>

- [15] Prósper, M.A., Otero-Casal, C., Fernández, F.C., Miguez-Macho, G. (2019). Wind power forecasting for a real onshore wind farm on complex terrain using WRF high resolution simulations. *Renewable Energy*, 135: 674-686. <https://doi.org/10.1016/j.renene.2018.12.047>
- [16] Malakouti, S.M. (2023). Prediction of wind speed and power with LightGBM and grid search: Case study based on Scada system in Turkey. *International Journal of Energy Production and Management*, 8(1): 35-40. <https://doi.org/10.18280/ijepm.080105>
- [17] Sward, J.A., Ault, T.R., Zhang, K.M. (2022). Genetic algorithm selection of the weather research and forecasting model physics to support wind and solar energy integration. *Energy*, 254: 124367. <https://doi.org/10.1016/j.energy.2022.124367>
- [18] Alzgool, M., Khalaf, A.A., Nasan, O., Khatabi, L., Alrifai, M.A. (2023). Design and simulation of a renewable energy-based smart grid for Ma'an City, Jordan: A feasibility study. *International Journal of Energy Production and Management*, 8(4): 219-227. <https://doi.org/10.18280/ijepm.080403>
- [19] Skamarock, W.C., Klemp, J.B., Dudhia, J., Gill, D.O., Barker, D.M., Duda, M.G., Powers, J.G. (2008). A description of the advanced research WRF Version 3. NCAR Technical Note, 475(125), 10-5065.
- [20] Colarossi, D., Principi, P. (2023). Optimal sizing of a photovoltaic/energy storage/cold ironing system: Life cycle cost approach and environmental analysis. *Energy Conversion and Management*, 291: 117255. <https://doi.org/10.1016/j.enconman.2023.117255>

NOMENCLATURE

A	Area, m ²
AMP	Alternative Maritime Power
C _P	Dimensionless wind turbine's power coefficient
f _{PV}	PV derating factor
G _t	Solar radiation, W/m ²
G _{T,STC}	Solar radiation at standard test conditions, W/m ²
GFS	Global Forecasting System
NCAR	National Center for Atmospheric Research
NOCT	Panel's operative temperature, °C
P _w	Output power of the wind turbine, kW
P _{pv}	Output power of the PV system, kW
P _r	Rated capacity of the PV plant, kW
PV	Photovoltaic
SoC	State of Charge, kWh
T _a	Air temperature
T _c	PV cell temperature, °C
T _{C,STC}	PV cell temperature under standard test conditions, °C
WRF	Weather Research and Forecasting
W _s	Wind speed, m/s

Greek symbols

α_p	PV temperature coefficient of power,
ρ	Air density, kg/m ³